CONF-7908101--1

THE ROLE OF INERT GASES IN FIRST WALL PHENOMENA IN FUSION DEVICES

by

S. K. Das

Prepared for

Symposium on

Inert Gases in Metals

Harwell, England

August 8-11, 1979

UofC-AUA-USDOE

ARGONNE NATIONAL LABORATORY, ARGONNE, ILLINOIS

Operated under Contract W-31-109-Eng-38 for the

U. S. DEPARTMENT OF ENERGY

Invited paper presented at the consultant symposium on "Inert Gases in Metals" held at AERE, Harwell, England August 8-11, 1979. (to appear in the proceedings)

The Role of Inert Gases in First Wall Phenomena in Fusion Devices*

S. K. Dast

Argonne National Laboratory, Argonne, Illinois, U.S.A.

ABSTRACT

The first wall surfaces of fusion devices will be exposed to bombardment by inert gaseous projectiles such as helium. The flux, energy and angular distribution of the helium radiation will depend not only on the type of device but also on its design parameters. For near term tokamak devices, the first wall surface phenomena caused by helium bombardment that appear to be quite important are physical sputtering and radiation blistering. Examples of these processes for a number of first wall candidate materials are discussed. While the physical sputtering phenomen is well understood, the mechanism of blister formation is still not fully understood. The various models proposed for radiation blistering of metal during helium bombardment is critically reviewed in the light of most recent experimental results.

1. INTRODUCTION

In a fusion device having D-T plasma energetic D, T, and He particles can leak out of the confining magnetic fields either as ions or as neutrals (formed, for example, by charge exchange near the plasma edge) and strike the first wall surfaces. The impact of such projectiles on surfaces can cause a variety of surface phenomena such as physical and chemical sputtering, radiation blistering, vaporization, desorption, and back scattering and has been reviewed by various authors [1-3]. In a fusion device the inert gas that plays a major role in the first wall phenomena is helium which is formed by the D-T fusion reaction. In this paper, the discussion will be limited to only the processes that are of great importance for the bombardment of first wall with helium projectiles. Two processes that appear to be quite important are physical sputtering and radiation blistering, particularly for near term tokamak devices. Both physical sputtering and radiation blistering due to helium irradiation can cause first wall surface erosion and contamination of the plasma with material eroded from the wall.

* Work performed under the auspices of U. S. Department of Energy

† Now at United Technologies Corporation, Pratt and Whitney Aircraft Group, West Palm Beach, Florida, U. S. A.

In order to estimate the extent of surface erosion and plasma contamination due to helium bombardment of first wall it is not only necessary to know the yields for the various processes but also the helium flux as a function of energy and angle of incidence. In the following section the helium particle fluxes expected to reach the first wall of fusion devices will be briefly described. This will be followed by a brief review of physical sputtering and a critical discussion of radiation blistering induced by helium bombardment.

2. HELIUM RADIATIONS STRIKING THE FIRST WALL

Significant differences in the estimated helium fluxes and their energy and angular distribution exist between the reactors of different confinement concepts. For example, both the mean energy and the flux of helium projectiles to first wall of a D-T mirror reactor have been estimated [4] to be more than an order of magnitude higher than the estimates for a tokamak reactor [5,6]. Furthermore, for inertially confined fusion reactors the helium radiations to the first wall will be significantly different from their magnetic confinement counter parts [7]. Even for tokamak devices the helium flux to first wall is expected to vary from one device to the other depending on the design parameters [8, 9]. In the near term tokamak devices (e.g. TFTR, ORNL-EPR, JEPR, T-20) with smaller radii and moderate confinement conditions a significant fraction (up to 20%) of the 3.5-MeV ^{4}He particles can reach the first wall with no appreciable loss in energy [8-10]. Thus the helium energy distribution reaching the first wall will have a delta function at 3.5 MeV. Figure 1 shows a typical He ion energy spectrum calculated for the Tokamak T-20 [11]. The low energy peak in the helium spectrum (Figure 1) is characteristic of the plasma-edge temperature (100-500 eV depending on the device) and will cause some surface erosion of first wall by physical sputtering but little damage due to blistering. On the other hand, the 3.5-MeV helium projectiles will contribute very little to physical sputtering and will be the major source of surface erosion due to blistering.

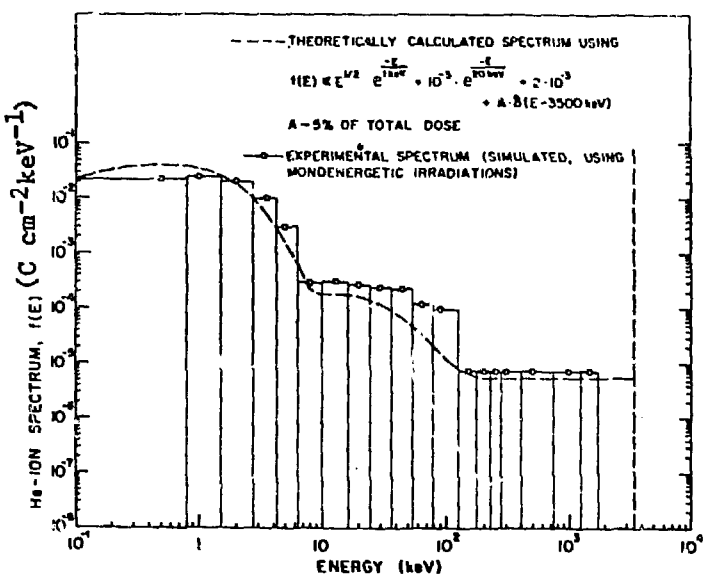

Figure 1. Double logarithmic plot of He ion spectrum (dashed line) per energy interval as a function of energy calculated for Tokamak T-20 first wall. Open squares show actual He energies that have been used to simulate theoretical spectrum [11].

The extent of surface damage will also depend on the angle of incidence of the helium projectiles striking the first wall. The low energy component characteristic of plasma edge temperature has a large angular spread and can be roughly assumed to be spatially isotropic whereas 3.5-MeV helium projectiles do not strike the first wall surface uniformly. It has been pointed out by Hively and Miley [8,9] and also by Bauer et al [10] that the wall loading profile in a tokamak is complicated by the banana like orbits of

the alpha particle, resulting in a highly peaked wall loading as a function of the poloidal angle. For a low β, axisymmetric tokamak operating in the collisionless regime, the 3.5-MeV alpha particle losses to the first walls of such tokamak devices as TFTR, EPR-1, and UWMAK-I occur either to the upper or lower half plane of the particular device, depending on the direction of the toroidal field. The significance of such angular distribution on first wall erosion due to blistering has been discussed recently by Fenske et. al. [12] and by Bauer et. al. [10].

3. PHYSICAL SPUTTERING DUE TO HELIUM RADIATIONS

The basic mechanism of physical sputtering is reasonably well understood. When energetic ions or atoms impinge on surfaces they initiate collison cascades within the solid and cause in turn the emission of atom and/or ions from the surface regions. This process releases not only impurities into the plasma region but also causes surface damage and erosion. Since detailed reviews on physical sputtering appeared elsewhere [13-16], only a few points relevant to helium bombardment of a fusion reactor first wall will be made here. The physical sputtering yields (i.e., the mean number of particles released from the surface per incident projectile) are proportional to the energy deposited into nuclear motion (proportional to nucler stopping power) near the surface and inversely proportional to surface binding energy [13-15]. The yield depends on a number of parameters such as the energy and angle of incidence of the projectiles, the atomic mass of both projectile and target atoms, the temperature and the surface condition. Unfortunately, the agreement between sputtering theory and experimental data is not satisfactory for the light projectiles like D, T, and He particularly at low energies (<10 keV), the calculated sputtering yields being much greater than experimental values [14-16]. Semiempirical relationships have been developed recently by Smith [16] which gives a reasonable agreement with available experimental data. It may be pointed out that there is very little data available for energies below 100 eV. Figure 2 shows some calculated [16] curves of physical sputtering yields for several materials, of interest to fusion reactor first wall, bombarded with monoenergetic helium ions. From these curves it can be seen that the position of the maximum in the energy dependent sputtering yield curve moves to higher energies as the mass of the target increases. More recently Bohdansky et.al. [17] have given an empirical relationship for energy dependence of light ion sputtering yields for a large number of ion-target combinations in the energy range of 50 eV to 50 keV.

Most of the helium sputtering yield data available to date are for monoenergetic ions and for normal incidence. However, as pointed out earlier the helium particles incident on the first wall will include a range of energies and incident angles. The experimental data on the angular dependence of sputtering yields for candidate fusion reactor materials is very limited. The energies of the helium particles striking the first wall can be assumed to be maxwellian [18]. The integrated physical sputtering yields for a large number of materials have been calculated by Smith [16] by averaging the calculated monoenergetic sputtering yields with Maxwellian distribution of incident particle energies. Thus knowing the plasma edge temperature the particle release from the first wall due to helium bombardment can be estimated reasonably well. For most devices helium particles in the 100-500 eV range (characteristic of plasma edge temperature, Figure 1) will contribute to some first wall erosion but will not be a serious problem because

the helium flux to the first wall is not expected to be very high. On the other hand, the fluxes of 3.5-MeV helium particles will be relatively higher but the erosion due to sputtering will be negligible because at the high energy the yields are extremely low (Figure 2). The first wall surface erosion due to physical sputtering will be dominated by sputtering due to D and T particle whose fluxes to the first wall are estimated to be more than an order of magnitude higher than the helium flux [1, 18].

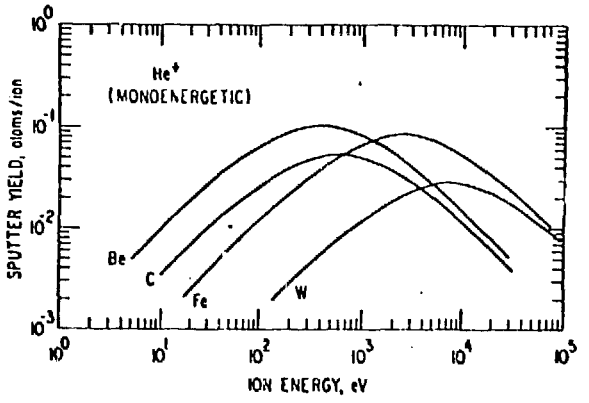

Figure 2. Calculated energy-dependent physical sputtering yields of fusion reactor first wall materials bombarded with monoenergetic helium ions 16 .

4. HELIUM BLISTERING

The irradiation of metal surfaces with energetic helium projectiles to sufficiently high doses has been known to cause blister formation on the surface under certain conditions. Since the phenomenon of radiation blistering in metals has been reviewed recently [19, 20] only some of the more recent developments on the mechanisms of blister formation and its role in surface erosion and plasma contamination will be discussed here. To date no blistering theory exists that can quantitatively predict important parameters required to evaluate the influence that blistering will have on plasma contamination. Several models have been proposed to explain the formation of surface blisters on helium-bombarded metal surfaces. These models can be classified into two broad categories: (a) gas pressure driven models [21-35] and (b) lateral stress driven models [36-39]. The gas pressure driven models can be subdivided into two, namely, (i) those based on bubble coalescence - interbubble rupture [23-31], and (ii) those based on percolation of helium in the lattice [33, 34]. Figure 3 illustrates the basic mechanisms involved in bubble coalescence - gas pressure (Figures 3a-3c) and lateral stress (Figures 3d-3f) models. According to the bubble coalescense models, as the incident helium ions slow down in the metal, they displace atoms from their lattice sites. The resulting vacancies and gas atoms combine with one another to form cavities in the matrix as depicted in Figure 3a. As the dose is increased, the density and/or size of the cavities increase to the point where coalescence occurs as shown in Figure 3b. Due to coalescence and the continued deposition of helium, the internal gas pressure within the cavities increases. This, together with a reduction in the effective load-bearing cross section due to volume swelling, increases the stress in regions between the cavities. Eventually, due to the combination of these two effects,

the ultimate tensile strength (or fracture strength) of the material is exceeded and the skin is plastically deformed and pushed upwards as shown in Figure 3c. In the integrated lateral stress model [37-39] it is suggested that the large lateral stresses introduced in the implanted layer leads to elastic instability and buckling of the implanted surface layer above the weakened interface region, and thus gas pressure is not the driving force behind the surface deformation. Figure 3d illustrates some major lattice imperfections in the implant region. The first step in surface deformation is the creation of a weakened interface region by shear yielding at stress concentration points (Figure 3e). Figure 3e shows the elastic plate equivalent for a diameter D of the weakened interface just below the point of elastic instability. Finally, Figure 3f shows the buckled plate after diameter D of weakened interface has exceeded the value where elastic instability can occur.

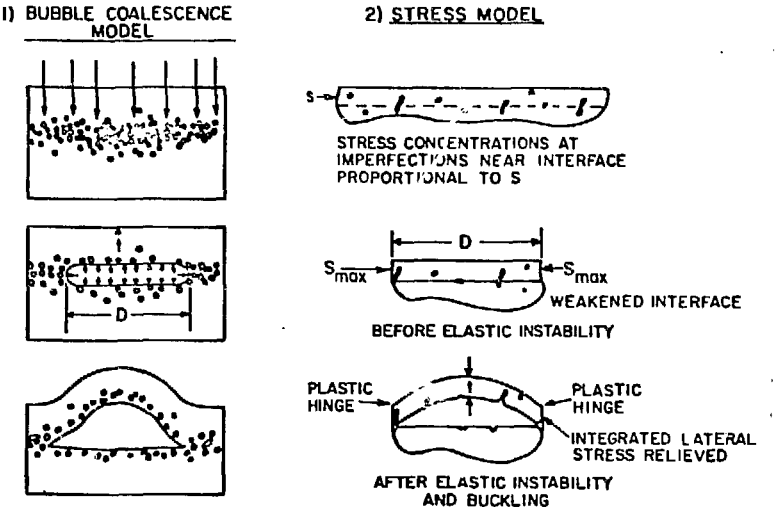

Figure 3. Schematic diagrams of (a-c) bubble coalescence - gas pressure model [19] and (d-f) lateral stress model [39] of blister formation in metals.

In the gas pressure models it is expected that the depth at which the skin separates from the bulk (blister skin thickness) should correspond to the peak in the projected range probability distribution (Figure 3c). This had been observed for a number of metals bombarded with helium ions with energies >60 keV [19]. However, subsequent measurements at low energies (<20 keV) showed the blister skin thicknesses to be no longer in good agreement with calculated average projected ranges. These observations led several groups to propose the lateral stress models which do not require the blister skin to separate at the peak in the projected range distribution [37-39]. These models assume that the shear stresses that initiate blister skin separation are proportional to the gradient of the volume swelling (and hence the projected range profile) or assume separation occurs at depths where the integrated lateral stress exceeds a critical value. As a first approximation, many of the proponents of lateral stress model assume the skin thickness, t, is equal to ($R_p + \Delta R_p$) where R_p is the average projected range and ΔR_p is the straggling in the projected range distribution. For high incident energies, ΔR_p is small compared to R_p and thus t is nearly equal to R_p. However, at low energies, ΔR_p is comparable in magnitude to R_p, and therefore t is predicted to be considerably larger than R_p.

Recent measurements on (a) depth distribution of helium bubbles by transmission electron microscopy [40, 41], (b) depth profile of helium concentration using Elastic Recoil Detection technique [42, 43] and Rutherford back

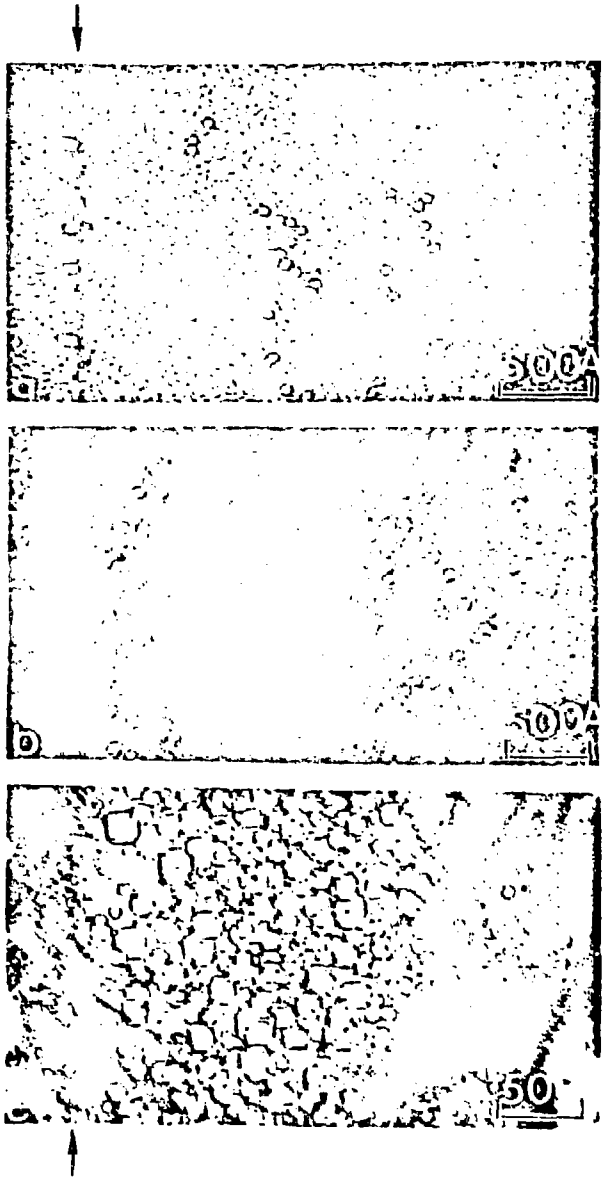

Figure 4. Transmission electron micrographs of annealed polycrystalline nickel irradiated at 500°C with 20-KeV $^4He^+$ ions for total doses of (a) 2.9 X 10^{15} ions/cm^2, (b) 2.9 X 10^{16} ions/cm^2, and (c) 2.9 X 10^{17} ions/cm^2. 40

scattering [44] and (c) surface expansion by optical interferometry [43, 45] clearly show that the descrepancy between the blister skin thickness measured by scanning electron microscopy and the calculated projected range for low energies (<20 keV) is in fact, due to the large swelling of the blister skin. A few examples of these measurements are given in the following. Using a transverse sectioning technique [46] complete depth distribution of helium bubbles in nickel has been measured. Figures 4a, 4b, and 4c show typical transmission electron micrographs of the plated and irradiated regions for an annealed polycrystalline nickel sample irradiated at 500°C with 20-keV $^4He^+$ ions to total doses of 2.9 X 10^{15}, 2.9 X 10^{16} and 2.9 X 10^{17} ions/cm^2, respectively. The interface between the plating and the irradiated region is marked by the vertical arrows. It can be seen in Figure 4 that with increasing dose, both the size and the number density of cavities (bubbles or voids) increase. Quantitative measurements of volume fraction of cavities (swelling) made from high magnification micrographs for depth intervals of 250 Å from surface, taking into account the measured variation in foil thickness [46] are shown in Figure 5a. Helium concentration profile measured for same type of sample using elastic recoil detection technique is also shown in this figure. It can be seen that within the limits of the experimental error the two profiles agree quite well. The curves in Figure 5b are the energy deposition and projected range profiles calculated [41] using the Monte-Carlo computer program TRIM developed by Biersack [47]. It may be pointed out that for low energies (<20 keV) most probable ranges calculated by the Monte-Carlo code give values that are 25-30% higher than those calculated [48] according to Brice or LSS which assume a Gaussian profile for the range distribution. For 20-keV He irradiation of nickel at 500°C the skin thickness measured by scanning electron microscopy give values of 0.11-0.16 μm [40] which compare favorably with the peak in the depth distribution of swelling and helium concentration, and calculated projected range distribution Figure 5.

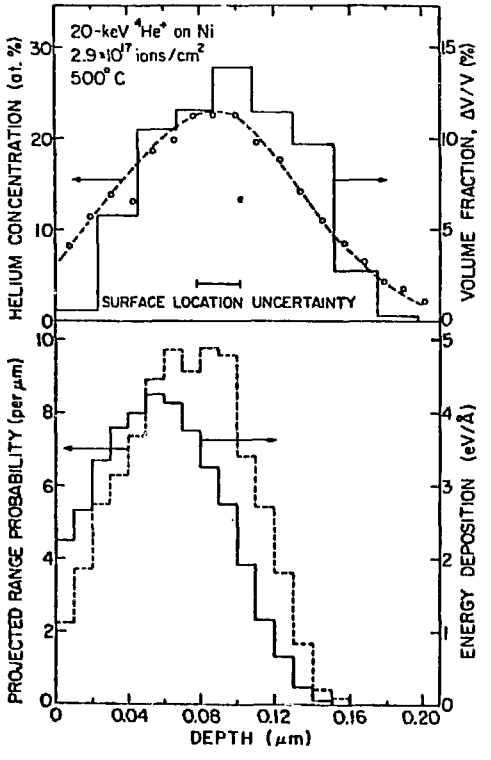

Figure 5. (a) The experimental depth distributions of volume fraction of cavities measured from Figure 4c and helium concentration measured by elastic recoil detection technique for nickel irradiated with 20-keV $^4He^+$ ions at 500°C to a dose of 2.9 X 10^{17} ions/cm^2. (b) The theoretical Monte Carlo projected range and energy deposition profiles for 20-keV $^4He^+$ ions in nickel [41].

Furthermore, recent measurements of surface displacement by optical interferometry by St. Jacques et al [43, 45] on low energy helium implantation of niobium, suggest that the swelling due to the helium bubbles can account for the discrepancy between the measured skin thickness and the calculated projected range. Figure 6 shows plot of surface displacement as a function of total dose for Nb irradiated with He ions of different energies. It is interesting to note that in the energy range (5-25 keV) investigated the surface displacement increases linearly with total dose independent of energy, indicating that swelling is proportional to helium concentration. The total swelling estimated from surface displacement measurements gives values that are larger than those measured using transmission electron microscopy [43]. This may in part due to the presence of helium bubbles or helium-vacancy clusters which are too small to be resolved in transmission electron microscope. Thus, the difference between observed blister skin thickness and calculated average projected ranges can be explained if one takes into account volumetric swelling of the skin and calculates the range profile properly e.g. using a Monte-Carlo code.

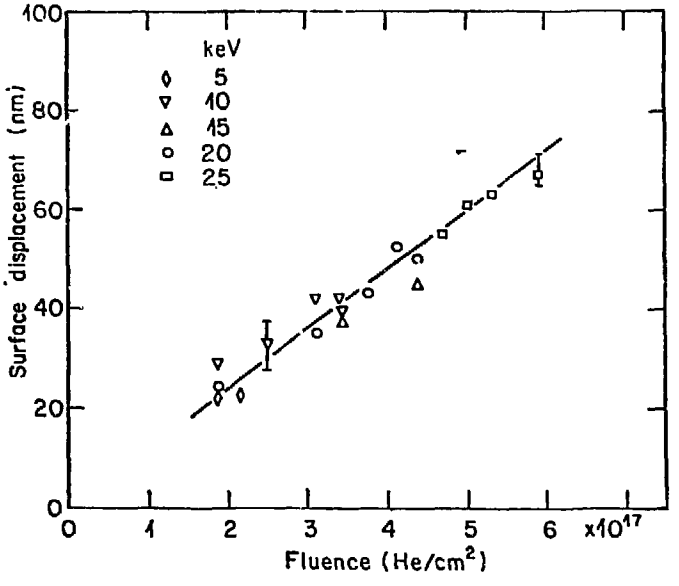

Figure 6. The experimental values of surface displacement as a function of total dose for Nb [43].

Furthermore, some measurements on depth distribution of helium bubbles in nickel has also been done for higher energy of 500 keV for different doses [48]. Figure 7 shows a plot of volume fraction (swelling), number density, and average diameter of cavities near the peak swelling region for 500-keV $^4He^+$ irradiated nickel as a function of total dose. These data show that the cavity density decreases and the cavity diameter increases sharply beyond a certain dose (Figure 6). These trends have been taken as direct evidence of helium bubble coalescence 48 as predicted by bubble coalescence models. It must be noted for the high irradiation temperature of 500°C coalescence occurs much before (at doses between 1 X 10^{17} and 5 X 10^{17} ions/cm^2) blisters appear (critical dose for blister appearance is 1 X 10^{18} ions/cm^2) on the surface. This may not necessarily be true for low temperature irradiations where vacancy mobility is very small and bubble growth may occur by punching out dislocation loops [28]. In such cases once the interbubble spacing has decreased to such a level that the excess gas pressure causes interbubble rupture between two neighboring bubbles and leads to the formation of penny shaped crack (Figure 3b) which forms blisters by gas driven surface deformation.

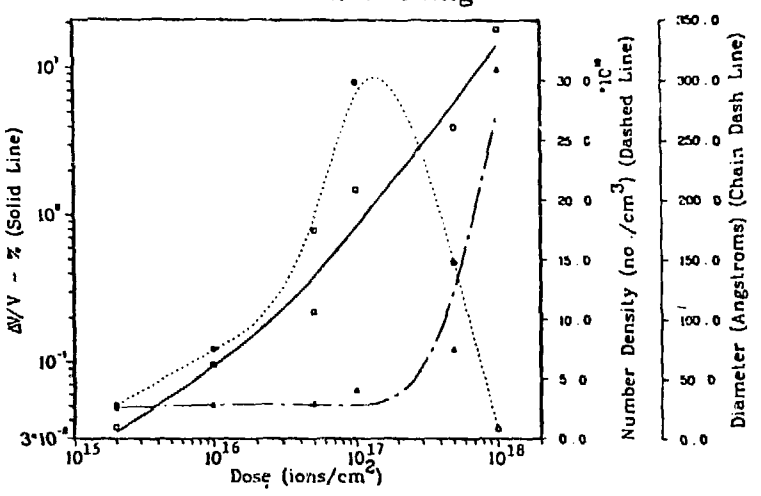

Figure 7. The cavity volume fraction (ΔV/V), density and average diameter at the peak swelling depth, as a function of total dose for nickel irradiated at 500°C with 500-keV $^4He^+$ ions. [48]

It is clear from the discussion above that all the gas pressure models assume that there is excess pressure in the helium bubbles which initiate interbubble rupture or coalescence. However, it is very difficult to measure gas pressure in the bubbles. Several estimations of gas pressure in the helium bubbes made form the experimentally determined bubble diameters [27, 28, 41, 48] indicate that the bubbles are overpressurized. For example, for the case of 500°C irradiation of nickel with 500-keV $^4He^+$ ions if one assumes that the cavities are equilibrium helium bubbles a maximum only 21% of the total implanted helium will be contained in all the visible cavities at a dose of 1 X 10^{18} ions/cm^2 (the critical dose for blister appearance for these irradiation conditions). Since measurements of helium concentration by elastic recoil detection technique show that for the above irradiation conditions 85-90% of the implanted helium is retained in the sample, there must be more than 21% of the implanted helium in the cavities (i.e. the cavities are overpressurized gas bubbles). Simple calculations of gas pressure needed to cause fracture in the interbubble region show that only 50-60% of the helium contained in the matrix is sufficient to obtain a pressure high enough to exceed fracture strength [48].

The proponents of lateral stress model have criticized the gas pressure models on the basis that it cannot explain a suggested relationship, $D \propto t^{1-5}$ between blister diameter, D, and blister skin thickness, t. This relationship was initially suggested by Roth [37] and later by Risch et.al. [38] for helium blisters in niobium. EerNisse and Picraux 39 considered this relationship to be valid also for other materials such as Be, Ti, V, Mo, Pd and 430 stainless steel. However, they had very few data points for some of the materials. In order to make such a correlation between D and t meaningful it is important to consider that the blister diameter depends on parameters such as raget temperature, total dose, target microstructure (e.g. cold-worked or annealed), and the crystallographic orientation of the surface of monocrystals. The influence of these effects on the correlation between D and t has been recently discussed [49]. Taking these factors into consideration, a systematic study of the correlation between blister diameter and skin thickness has been done for helium blistering of an hcp metal, Be; an fcc metal, Ni; and two bcc metals, V and Nb, for helium ion energies in the range from 15 to 500 keV [49-51]. Figure 8 shows a summary of these results. A power curve fit [49] of D_{mp} (μm) with mean blister skin thickness, t (μm) gave the relationship $D_{mp} = 10.3\ t^{1.22}$ for Nb, $D_{mp} = 24.6\ t^{1.25}$ for Be, $D_{mp} = 12.4\ t^{1.15}$

for Ni, and $D_{mp} = 6.3\ t^{0.85}$ for V as shown in Figure 8. It is interesting to note that the exponent in the power relationship for Nb, Be and Ni is closer to 1.2 but for V it is less than unity. Furthermore, the D-t relationship has been found to be dependent on the irradiation temperature; for Nb irradiated at 700°C the relationship is $D_{mp,\ 700^{\circ}C} = 5.3\ t^{1.05}$ as compared to the relationship of $D_{mp,R.T.} = 10.3\ t^{1.22}$ for room temperature irradiation [49]. These results are in contrast to the prediction of stress model which gives the relationship $D \propto t^{1.5}$ independent of material and irradiation temperature. The material dependent parameters are contained only in the pre-exponential term.

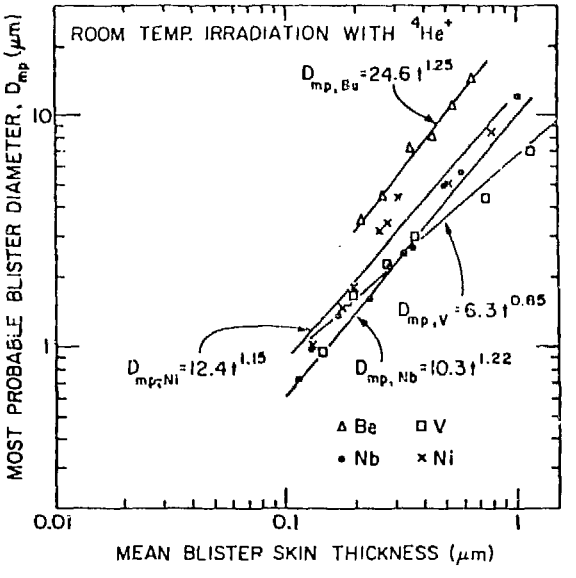

Figure 8. Double logarithmic plot of D_{mp} against t for helium blistering of some metals.

Recently Kamada and Higashida [31] have explained the D-t relationships obtained by Das et.al. 49-51 using a fracture model of blister formation. The model is based on the growth of a microcrack (driven by internal gas pressure) nucleated at a depth near the projected range of ions. Using the linear elasticity theory, they calculated the radius of the plastic zone ahead of crack tip r, as a function of internal gas pressure p, within the crack, yield strength of material σ_y blister skin thickness t, crack radius r, and the stress intensity factors. The dome-shaped blister is formed when the surface layer over the crack suffers general yielding, which may occur when the boundary of the plastic zone touches the surface of the material (i.e. r = t). Two factors are separated theoretically to be responsible for blister formation, one is related to only the geometry of the bubble and the other factor is related to physical and chemical properties of the injected helium and of the target material i.e. proportional to (p/σ_y). They showed that the factor p/σ_y is responsible for the non-linear relationship, $D \propto t^n$ and showed why n>1 for Ni and Be but <1 for V as has been experimentally observed. Thus, blistering models based on gas pressure can account for most of the experimentally observed D-t relationships, whereas the lateral stress models cannot. Furthermore, recent results by Evans and Eyre [52] on thin molybdenum samples irradiated with 100-keV He ions show that blisters can form on the rear surface (opposite to the implanted surface) an observation which is incompatible with the lateral stress model. Some additional experimental observations such as formation of nearly spherical blisters in helium irradiated vanadium under certain conditions [51] cannot be caused by elastic buckling of the implanted layer as invoked in the stress model but must re-

sult from surface deformation by internal gas pressure. On the other hand vertically elongated blisters have been observed in high displacement damage environments (e.g. Pt-10% Rh surfaces exposed to ^{252}Cf α-particles and fission fragments) which are difficult to explain by only the lateral stress or only the gas pressure model [53].

In the following the role helium blistering in surface erosion and plasma contamination of a D-T fusion reactor will be briefly discussed. It has been often argued by some authors that blistering may only be a transient phenomenon and not necessarily be a serious problem in a fusion reactor [2, 54 55]. It is known [56, 57] that helium blistering of metals (e.g. Nb) in the low energy range (<20 keV) disappears for sufficiently high doses ($6 \times 10^{18} - 2 \times 10^{19}$ ions/cm^2) due to the significant surface erosion by sputtering. However, in the high energy range (>100 keV) repetitive blister exfoliation of the irradiated surface occurs [58]. As discussed earlier (Sec. 2) for the next generation of D-T tokamak devices, a significant fraction of the helium flux will have an energy of 3.5 MeV. If the angular distribution fo these 3.5-MeV helium particles is taken into account most of them will be implanted at a depth of 1-2 μm in a stainless steel first wall [10]. This is the range where continuous blister exfoliation can be expected. However, the first wall is also being simultaneously bombarded by D and T projectiles whose total fluxes can be one to two orders of magnitude higher than the helium flux. This problem of blister formation under simultaneous D and T sputtering has been only recently analyzed [10, 12]. The results show that whether blistering will be significant process or not depends strongly on the D, T, and He flux and the plasma device parameter (e.g. plasma edge temperature) and the first wall material assumed. For example, assuming a D + T flux of 7.5×10^{14} ion/(cm^{2}S) and 3.5-MeV He flux of 1×10^{12}/(cm^{2}S) striking a stainless steel first wall, blistering will occur for plasma edge temperature of 60 eV, will be marginal for 200 eV and will not occur for 1 keV, but for a higher helium flux of 3×10^{12} ions/(cm^{2}S) blistering will definitely occur for plasma edge temperature of 200 eV [10]. Thus, whether helium blistering will be a dominant first wall process or not will strongly depend on device parameters. For near term tokamak devices with poor alpha confinement blistering will most likely be a problem, whereas it may not be so for future large reactors with better alpha confinement.

CONCLUDING REMARKS

In the past several years considerable understanding of the role of helium in the first wall phenomena of fusion devices has been obtained, particularly on the mechanisms of helium blistering. Recent results on correlation of blister with skin thickness together with the measurements on volume swelling in the blister skin using transmission electron microscopy and surface displacement techniques clearly indicate that blistering models based on bubble coalescence followed by gas pressure driven deformation provide an accurate description of the mechanisms in blistering. To date most of the relevant information on helium bombardment of candidate first wall materials have been obtained using monoenergetic ion beams. In a fusion reactor, however, the first wall surfaces will be bombarded simultaneously with other particles and photons having broad energy and angular distributions, that may give rise to synergistic effects. Future studies should be concentrated on the studies of helium irradiation during simultaneous bombardment with other projectiles and photons expected in the fusion reactor environment.

ACKNOWLEDGEMENTS

I am grateful to my former colleagues Dr. M. Kaminsky and Dr. G. Fenske for many valuable discussions on the topic. I would like to thank Dr. B. Terreault for his permission to quote his results prior to publication.

REFERENCES

1. M. Kaminsky, CRC critical Review in Solid State Sciences 6 (1976) 433.
2. R. Behrisch, J. Physique 38 (1977) 3.
3. W. Bauer, J. Nucl. Mat. 76 & 77 (1978) 3.
4. G. M. McCracken and P. E. Stott, Nucl. Fusion 19 (1979) 889.
5. J. Lee, J. Nucl. Mat. 53 (1974) 76.
6. G. Kulcinski et. al., J. Nucl. Mat. 53 (1974) 31.
7. T. O. Hunter and G. Kulcinski, J. Nucl. Mat. 76 & 77 (1978) 383.
8. L. M. Hively and G. H. Miley, Nucl. Fusion 17 (1977) 1031.
9. G. H. Miley and L. M. Hively, J. Nucl. Mat. 76 & 77 (1978) 389.
10. W. Bauer, K. L. Wilson, C. L. Bisson, L. G. Haggmark and R. J. Goldston, Nucl. Fusion 19 (1979) 93.
11. M. I. Guseva, V. Gusev, Yu. V. Martynenko, S. K. Das, and M. Kaminsky, First topical Meeting on Fusion Reactor Materials, Miami Beach, January 1979, J. Nucl. Mat. (in press).
12. G. Fenske, L. Hively, G. Miley and M. Kaminsky, J. Nucl. Mat. (in press).
13. P. Sigmund, Phys. Rev. 184 (1969) 383
14. R. Weissmann and P. Sigmund, Rad. Effects 19 (1973) 7.
15. H. F. Winters, Adv. in Chemistry 158 (1976) 1.
16. D. Smith, J. Nucl. Mat. 75 (1978) 20.
17. J. Roth, J. Bohdansky and A. P. Martinelli, to appear in Proc. of International Conference on Ion Beam Modification of Materials, Budapest, hungary September 1978.
18. W. Stacey, Jr. et. al. Argonne National Laboratory, ANL/CTR Rep. 76-3 (1976)
19. S. K. Das and M. Kaminsky, Advances in Chemistry 158 (1976) 113.
20. M. Kaminsky and S. K. Das, to appear in Proceedings of IXth Summer School and Symposium on the Physics of Ionized Gases, Dubrovnik, Yugoslavia, August 1978.
21. M. Kaminsky, Adv. in Mass Spectrometry 3 (1964) 69.
22. W. Primak and J. Luthra, J. Appl. Phys. 37, (1966) 2287.
23. R. S. Blewer and J. Maurin, J. Nucl. Mat. 44, (1972) 260.
24. S. K. Das and M. Kaminsky, J. Appl. Phys. 44, (1973) 25
25. S. K. Das and M. Kaminsky, Proc. Third Conf. Appl. of Small Accelerators, Vol. 1, ed. J. L. Duggan and I. L. Morgan, CONF-741040-P1 (USERDA Tech. Info. Center, Natl. Info. Serv. Springfield, VA 278 (1974)
26. G. M. McCracken, Japan J. Appl. Phys. Suppl. 2, Pt. 1, (1974) 269
27. J. H. Evans, J. Nucl. Mat. 61, (1976) 1.
28. J. H. Evans, J. Nucl. Mat. 68, (1977) 129 and also 76 & 77 (1978) 228.
29. O. Auciello, Radiation Effects, 30 (1976) 11.
30. B. Terreault, R. G. St-Jacques, G. Veilleux, J. G. Martel, J. L. Ecuyer, C. Brassard, and C. Cardinal, Can. J. Phys. 56 (1978) 235.
31. K. Kamada, and Y. Higashida, J. Appl. Phys. 50 (1979) 4131.
32. Yu V. Martynenko, Fiz. Plasmy 3 (1977) 697.
33. W. D. Wilson, C. L. Bisson and D. E. Amos, J. Nucl. Mat. 53, (1974) 154.
34. M. I. Baskes and W. D. Wilson, Radiation Effects 37 (1978) 93.
35. G. J. Thomas and W. Bauer, Radiation Effects, 17 (1973) 221.

36. Behrisch, J. Bottiger, W. Eckstein, V. Littmark, J. Roth and B.M.U. Scherzer, Appl. Phys. Lett. 27, (1975) 199.
37. J. Roth, Appl. of Ion Beams to Materials, eds. G. Carter, J. S. Colligon, and W. A. Grant (Inst. of Physics, London 1976) p. 280.
38. M. Risch, J. Roth and B.M.U. Scherzer, Plasma-Wall Interactions, (pergamon, 1977) p. 391.
39. E. P. EerNisse and S. T. Picraux, J. Appl. Phys. 48 (1977) 9.
40. G. Fenske, S. K. Das, M. Kaminsky and G. H. Miley, J. Nucl. Mat. 76 & 77 (1978) 247; Trans. Am Nucl. Soc 28 (1978) 196; and J. Nucl Mat (in press)
41. G. Fenske, Ph. D. Thesis Univ. of Illinois, Urbana, Illinois (1979).
42. G. Ross and B. Terreault, 8th International Conference on Atomic Collision in Solids, Hamilton, Canada, Aug. 1979, to appear in Nucl. Instr. and Methods.
43. R. G. St-Jacques, G. Veilleux and B. Terreault, in Ref. 42.
44. M. Braun, J. L. Whitton and B. Emmoth, Proc. First Topical Meeting on Fusion Reactor Materials, Miami Beach, January 1979, J. Nucl. Mat. (in press)
45. R. G. St-Jacques, G. Veilleux, J. G. Martel and B. Terreault, Proc. Int. Conf. Ion Beam Modification of Materials, Budapest, Hungary, Sept. 1978, to appear in Radiation Effects
46. G. Fenske, S. K. Das and M. Kaminsky, J. Nucl. Mat. 80 (1979) 373.
47. J. Biersack, Hahn-Meitner-Institute, Berlin, W. Germany, private communication (1979)
48. G. Fenske, S. K. Das, M. Kaminsky, and G. Miley, in Proc. of 8th International Conference on Atomic Collisons in Solids, Hamilton, Canada, Aug. 1979, to appear in Nucl. Instr. and Methods.
49. S. K. Das, M. Kaminsky, and G. Fenske, J. Apply. Phys. 50 (1979) 3304.
50. S. K. Das, M. Kaminsky and G. Fenske, J. Nucl. Mat. 76 & 77 (1978) 215.
51. M. Kaminsky and S. K. Das, J. Appl. Phys. 49 (1978) 5673.
52. J. H. Evans and B. L. Eyre, J. Nucl. Mat. 67 (1974) 307.
53. W. R. McDonell, J. Nucl. Mat. 76 & 77 (1978) 258-260.
54. R. Behrisch, M. Risch, J. Roth and B.M.U. Scherzer, Proceed. 9th Symp. on Fusion Tech. (Pergamon 1976) p. 531.
55. B.M.U. Scherzer, R. Behrisch and J. Roth, Plasma-Wall Interaction (Pergamon, 1977) 353.
56. J. G. Martel, R. St-Jacques, B. Terreault, G. Veilleux, J. Nucl. Mat. 53 142 (1974).
57. J. Roth, R. Behrisch and B. M. Scherzer, J. Nucl. Mat. 57, 365 (1975).
58. M. Kaminsky and S. K. Das, J. Nucl. Mat. 76 & 77 (1978) 256.